Journal of Macromolecular Science, Part A
Publication details, including instructions for authors and subscription information:
http://www.informaworld.com/smpp/title~content=t713597274

Electric Charge Scavenger Effects in PMMA Photopolymerization Initiated by TiO_2 Semiconductor Nanoparticles

Jin Ye[a]; Xiuyuan Ni[a]; Ceng Dong[a]
[a] Department of Macromolecular Science, The Key Laboratory of Molecular Engineering of Polymer, State Educational Minister, Fudan University, Shanghai, P.R. China

To cite this Article Ye, Jin , Ni, Xiuyuan and Dong, Ceng(2005) 'Electric Charge Scavenger Effects in PMMA Photopolymerization Initiated by TiO_2 Semiconductor Nanoparticles', Journal of Macromolecular Science, Part A, 42: 10, 1451 — 1461
To link to this Article: DOI: 10.1080/10601320500207612
URL: http://dx.doi.org/10.1080/10601320500207612

Journal of Macromolecular Science®, Part A: Pure and Applied Chemistry, 42:1451–1461, 2005

ISSN 1060-1325 print/1520-5738 online
DOI: 10.1080/10601320500207612

Electric Charge Scavenger Effects in PMMA Photopolymerization Initiated by TiO_2 Semiconductor Nanoparticles

JIN YE, XIUYUAN NI, AND CENG DONG

Department of Macromolecular Science, The Key Laboratory of Molecular Engineering of Polymer, State Educational Minister, Fudan University, Shanghai, P.R. China

The photopolymerization of methyl methacrylate through changing the initiating species from TiO_2 semiconductor nanoparticles was studied in this paper. By using the hole or electron scavenger added into the polymerization systems, we found that there were two initiation pathways depending on the reaction modes. Methods such as GPC, TGA, DSC, H-NMR were performed to characterize the polymer and composites. We found that by different reaction modes the polymer obtained had the obvious distinguishing molecular weights, molecular structure of polymer, thermal degradation temperature and glass transition temperature (Tg). The effects of the electric charge scavengers on the photopolymerization were discussed.

Keywords photopolymerization, semiconductors, photocatalysis, TiO_2, charge scavenger, polymer characterization

Introduction

Photocatalysis of semiconductors has found important applications in the fields like photocatalytic degradation of pollutants (1), high performance solar-cells (2) and photoinduced hydrophilic surfaces (3). There also have been some reports on semiconductor initiated photopolymerizations since it was introduced in 1961 (4–8). Recently, we have developed a new polymerization technique of photo-assisted polymerizations initiated by nano-TiO_2 semiconductors (9). The heterogeneous polymerizations were carried out by dispersing the TiO_2 particles into MMA aqueous solutions. UV light at 365 nm was employed to stimulate photocatalysis of the semiconductors. Self-polymerization of vinyl monomers cannot work under this irradiation condition. The polymerization was found to occur on the semiconductor surfaces, leading to nanocomposites composed of nano-TiO_2 particles enwrapped by polymers. The analysis with various instrumental tools implied a double-species initiation in the polymerization. It has been proposed that both the valence-band hole (h^+_{vb}) and OH-radical can work as initiators (9).

Received November 2004, Accepted March 2005
Address correspondence to Xiuyuan Ni, Department of Macromolecular Science, The Key Laboratory of Molecular Engineering of Polymer, State Educational Minister, Fudan University, Shanghai 200433, P.R. China. E-mail: xyni@fudan.edu.cn

The polymerization technique from our laboratory offers not only a novel way to gain the situ-growing nanocomposites, but also a good joint to many promising applications, especially semiconductors interfacing polymers for light emission and electrical conductive materials (10). We currently concentrate on controlling the polymerization progress and thus the structures of the resulted polymers.

The present study is, taking PMMA as a model polymer, to investigate controlling the polymerization through changing the initiation pathways of nano-TiO_2. The change of the initiation pathways is explored by adding the hole and electron scavengers, respectively. The reason for choosing PMMA as a model polymer is that the physicochemical nature of PMMA has been comprehensively understood. It may enable one to conclude precisely how the polymer structures depend on the initiation pathways.

Due to the fact that the presence of methanol initiates efficient hole transfer from the oxygen lattice to the methanol, methanol has been widely used as the hole scavenger of TiO_2 photocatalysis (11–13). Effects of Cu(II) ions on TiO_2 photocatalysis have been studied by many authors (14, 15). They all believed a mechanism of electron capturing at the semiconductor surface by the Cu(II) irons. This paper uses methanol and cupric nitrate as the hole scavenger and the electron scavenger, respectively.

Experimental

Materials

The nano-TiO_2 semiconductors used was Degussa P25 (80% anatase and 20% rutile) with an average diameter of 21 nm. All the chemicals used were of analytical reagent grade. MMA, methanol and tetrachlorofluorescein (THF) were distilled before use. Deionized water was used in the experiments.

Photopolymerization

The experiments were conducted in the procedures described in details in our previous work (9). In this study, the feed concentration of the monomer was 10.35 g/L, the content of nano-TiO_2 was 1 g/L. The polymerizations were carried out in three different modes: without charge scavenger; adding methanol as the hole scavenger at a concentration of 1% v/v; adding cupric nitrate as the electron scavenger at a content of 0.1 mol/L. The resulting sample corresponding to each mode was named as Sample A, B and C, respectively. The reaction mixture was stirred throughout the course of the 5 hours' reaction to prevent precipitation of the reactants.

The composite products were separated from the reacted system by ultra centrifugation, washed by water and dried under vacuum. THF was then used to dissolve PMMA from the TiO_2 particles, followed by ultra centrifugation to remove TiO_2 from the solution. The process was repeated three times. Then the pure polymer solution was dried under vacuum to eliminate the solvent.

Characterization

Molecular weights of the polymer obtained were measured by GPC (HP Aligent 1100) and calibrated by standard polystyrenes. TGA was performed on a Perkin–Elmer Pyris 1 TGA instrument at a heating rate of 10°C/min under nitrogen atmosphere. Tg of the polymers

were determined using a Perkin–Elmer Pyris 1 DSC analyzer. ^{1}H-NMR spectra were recorded on a Bruke DMX500 spectrometer at 300 K using $CDCl_3$ as solvent.

Results and Discussion

GPC

Figure 1 shows typical GPC drawings of Samples A, B and C. As described earlier, they are prepared without charge scavenger, adding methanol as the hole scavenger and cupric nitrate as the electron scavenger, respectively. It is interesting to find that the GPC trace of Sample A displays a clear bimodal-distribution, whereas that of both Sample B and C shows a mono-peak distribution. The results clearly indicate the effects of the added charge scavengers on the molecular weights and molecular weight distributions of the resulting polymer. It is observed that Sample B is at the high M_w region, while Sample C at the low M_w region. If we overlap, add the GPC traces of the two samples, a bimodal distribution can be obtained similar to that of Sample A. Several studies on the semiconductor initiated photopolymerizations have reported that the polymers synthesized have such a bimodality of molecular weights (4–6). However, profound explanations were not made without comparable experimental results. Considering the GPC features of Sample B and C in this paper and the opinions in the literature, we can provide a more sound explanation: the polymerization in the presence of the hole scavenge, progresses in a different reaction mechanism from that with the electron scavenge; the polymerization without any charge scavenger has both of them. It can be also observed from Figure 1 that each peak of Sample A shifts to a lower molecular weight compared to the corresponding peaks of Sample B and C. These details indicate that the mechanisms coexistent in the polymerization may be not simply separate, but competitive. Meanwhile, these nanocomposite materials with different molecular weight distributions of polymer can lead to some various useful ways for applications.

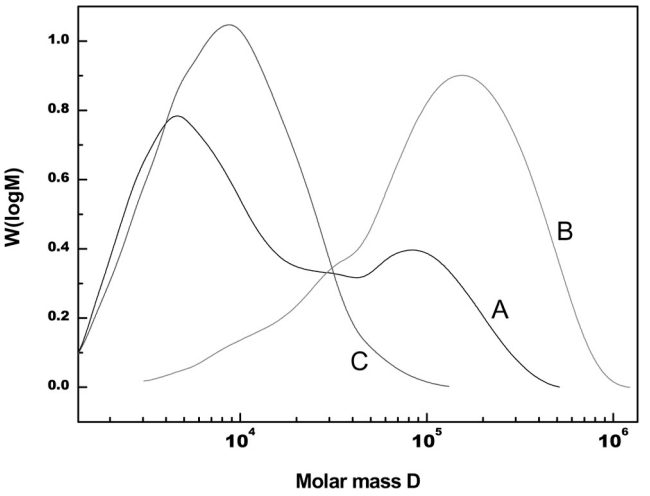

Figure 1. GPC traces of three reaction modes: (A) without charge scavenger; (B) adding hole scavenger; (C) adding electron scavenger.

Table 1
Molecular weights of PMMA prepared by different synthesis methods

Synthesis methods	$M_n \times 10^4$	$M_w \times 10^4$	PD	Monomer conversion
Without charge scavenger (A)	0.66	3.83	5.84	55.47%
Adding hole scavenger (B)	5.22	17.14	3.28	35.05%
Adding electron scavenger (C)	0.60	1.20	1.99	69.41%

The concentration of the monomer was 10.35 g/L and the nano-TiO_2 was 1 g/L. The incident light intensity was 12.7 mw/cm^2.

Table 1 shows that Sample B prepared by adding the hole scavenger has the highest molecular weight of the three samples, whereas Sample C prepared by adding the electron scavenge has the opposition. The molecular weight of Sample B is nearly decuple as more as that of Sample C. The high polydispersity for Sample A is of course due to the different mechanisms coexistent in the polymerization. It is also found that the polymerization in presence of the electron scavenger performs the highest monomer conversion and that with the hole scavenger has the opposition. The changes in the polymerization efficiency are related to effects of the charge scavenges on the photocatalysis of the TiO_2 semiconductors.

TGA

Previous studies have shown that the monomer is the chief product of the thermal decomposition of PMMA (16, 17). It was well accepted that TGA method can provide information concerning the reaction mechanism of MMA polymerization. The thermal degradation of normal free-radical polymerized PMMA is found to take place in three distinctive stages (7). These are approximately at 180, 230, and 390°C, respectively. The first is due to the scission of head-to-head linkages. The second is due to initial β-scission at vinylidene chain ends followed by unzipping. The last is due to the depolymerization initiated by random scission of main-chain C–C. It can immediately be seen from Figure 2, that mass loss occurring at various temperatures are significantly different from each other. The sample D is made by the normal free radical polymerization using H_2O_2 as the initiator for the comparison.

The differences become even more obvious when the derivative thermogravimetic (DTG) curves are examined (Figure 3). It can be found that each sample has the various stages of mass-loss degradation. The mass loss at 180°C for sample B is the most abundant of the four samples, however, that of Sample C has the least. Since the more (or less) head-to-head linkages can lead to a high (or low) tacticity, this result can confirm the conclusion of NMR described later.

We can also find a new peak at about 300°C compared with the sample D. The peak was identified to result from scission of the bond βCH_2-CH_2 to the terminal double formed during valence-band hole initiation (7, 9). The decomposition at this temperature represents the special structure of polymer by hole initiation mechanism. Sample C has a more abundant mass loss at this temperature compared with sample A and sample B. It is clear that the hole initiation rules the dominant status when the electron scavenger is added into the reaction system.

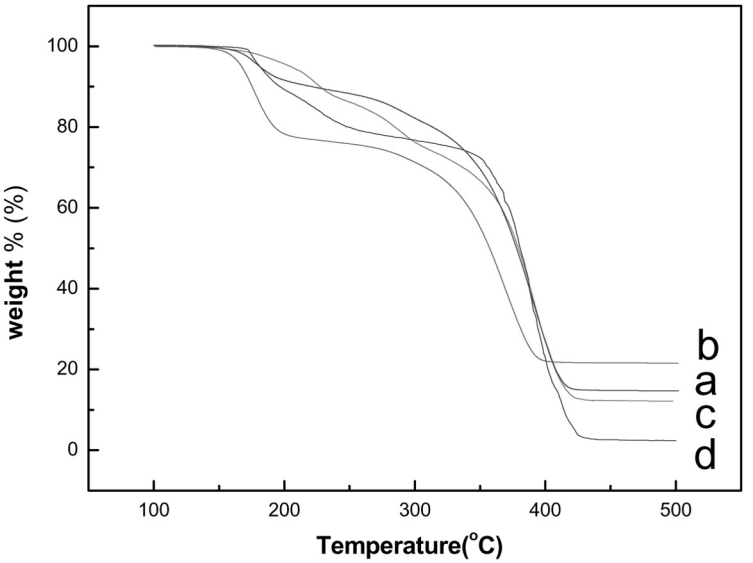

Figure 2. TGA curves of different sample: (a) without charge scavenger, (b) adding hole scavenger methanol, (c) adding electron scavenger cupric nitrate, (d) free radically using H_2O_2 as the initiator.

DSC

Figure 4 shows the DSC curves of the three samples. Sample A behaves as two glass transitions at nearly 80°C and 120°C, respectively. Both Sample B and C have signal glass transition around 120°C and 90°C, respectively. In view of the Fox-Flory relationship

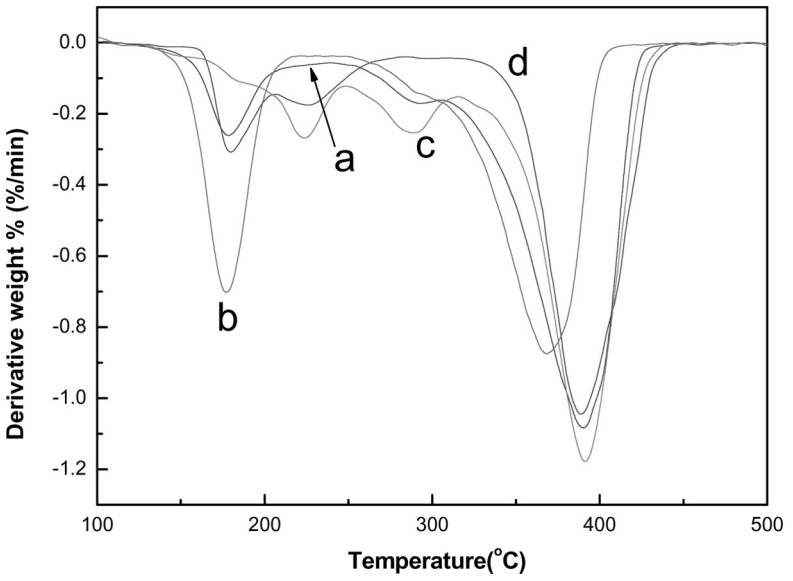

Figure 3. DTG curves of different samples: (a) without charge scavenger, (b) adding hole scavenger methanol, (c) adding electron scavenger cupric nitrate, (d) free radically using H_2O_2 as the initiator.

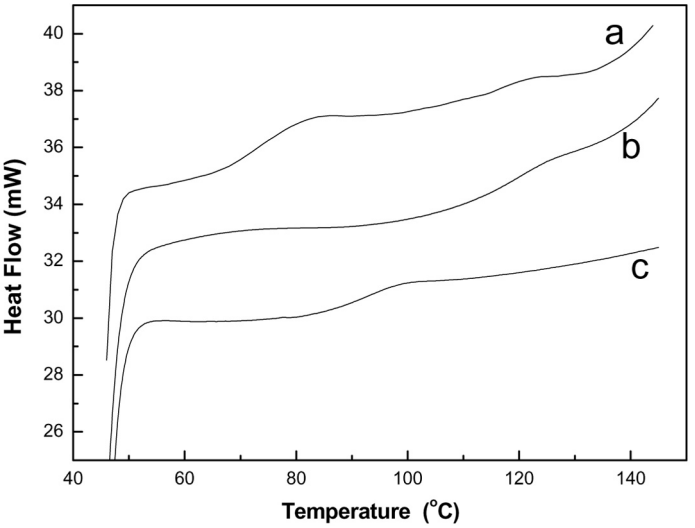

Figure 4. DSC traces of the three reaction modes at a heating rate of 20°C/min. (A) without charge scavenger, (B) adding hole scavenger and (C) adding electron scavenger.

between molecular weight and Tg (18, 19), the appearance of two glass transitions in Sample A results from two kinds of polymers, having different molecular weights, coexisting in the sample. It is in good agreement with the GPC results.

^{1}H-NMR

The ^{1}H-NMR spectra of Sample A and C are shown in Figures 5 and 6. The spectrum of Sample B is not shown for its similarity to Sample A. The signals assigned to α-methyl hydrogen ($-CH_3$) are in the 0.7–1.3 ppm range. The positions of the mm (isotactic), mr (heterotactic) and rr (syndiotactic) triads (20) are marked on the spectrum. Table 2 gives the abundance of the individual triads. The features of the samples stereoregularity indicate the nature of radical mechanism. Nevertheless, Sample C shows a more regular tacticity and Sample B shows a less one. It is associated with different initiation pathways occurring.

The main peaks corresponding to the methylene hydrogen ($-CH_2-$) and the methoxy hydrogen in bulk ($-OCH_3$) have been identified at $\delta = 1.3–2.2$ ppm and $\delta = 3.5–4.0$ ppm, respectively (21–23). In the spectrum of Sample C, there is a pair of two small peaks at $\delta = 4.3–4.4$ ppm range. Other authors have already identified the signals in the 4.3–5.0 ppm range as unsaturated chain end of the polymer (24–26). Hence, we consider the two peaks as corresponding to the different configuration of double bond endgroup. It is also important to find that each of the samples shows a peak at about $\delta = 8.4$ ppm. The peak is considered of the hydroxyl endgroup ($-OH$) because the peak disappears in the case of heavy water (D_2O) exchanging. The chemical shift of the hydrogen is somewhat higher than the normal ones, probably due to the effect of hydrogen bonds. The above information drawn is important evidence for the initiation mechanism that we will describe later.

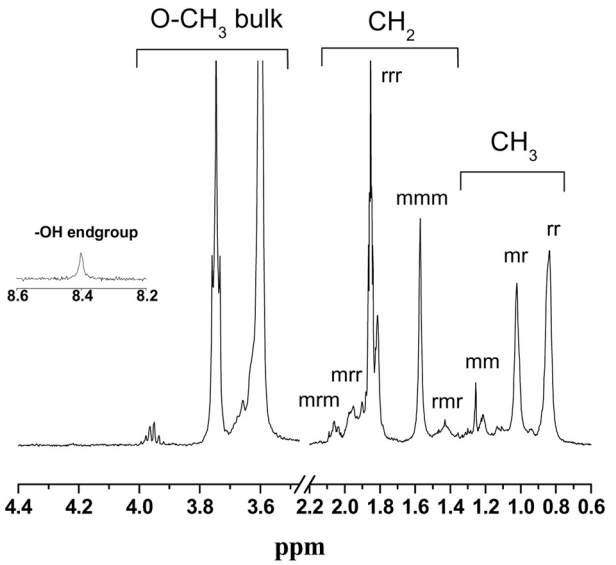

Figure 5. [1]H-NMR spectrum of Sample A.

Discussions on the Effects of Charge Scavengers

It is known that h_{vb}^{+} and simultaneously e_{cb}^{-} will be produced on the surface of TiO_2 semiconductors upon the UV illumination.

$$TiO_2 + hv \longrightarrow e_{cb}^{-} + h_{vb}^{+} \tag{1}$$

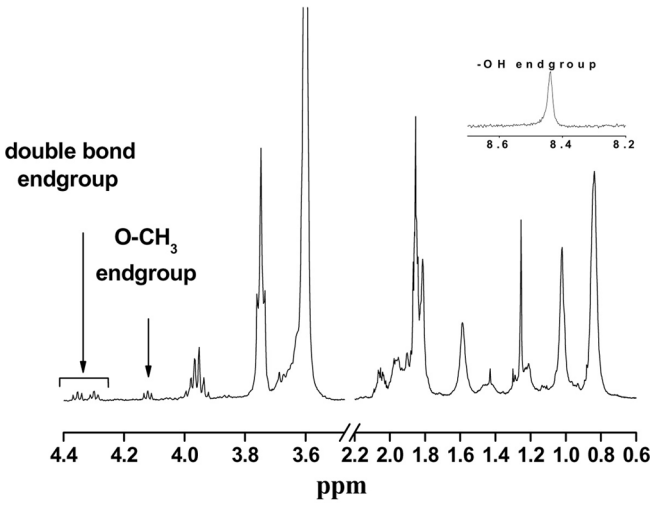

Figure 6. [1]H-NMR spectrum of Sample C.

Table 2
The abundance of the triads assigned to the α-methyl hydrogen

	Configurational sequences (%)		
Synthesis methods	mm	mr	Rr
Without charge scavenger	17.1	39.6	43.3
Adding hole scavenger	12.8	36.4	50.8
Adding electron scavenger	22.6	33.3	44.1

The concentration of the monomer was 10.35 g/L and the nano-TiO_2 was 1 g/L. The incident light intensity was 12.7 mw/cm^2.

The valence-band hole h_{vb}^+ of an excited TiO_2 particle can abstract a hydrogen atom from the MMA and produce a MMA radical (7, 9). The monomer radical can react with another MMA molecule to give a propagating radical. The process is described as follows:

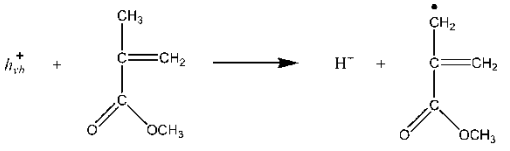

(2)

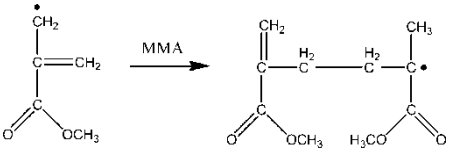

(3)

As a result, the polymer has a terminal double bond and the β bond is a $CH_2{-}CH_2$ (9). When the electron scavenger is added, e_{cb}^- is captured at the semiconductor surface by the Cu(II) irons (12, 13).

$$Cu^2 + e_{cb}^- \longrightarrow Cu^+ \tag{4}$$

In this case (Sample C), the initiation usually processes in this way. That is why we can find the unsaturated chain end signals in the 4.3–4.4 ppm range in the sample spectrum.

However, the initiation directly by the hole, is not the sole pathway, because the hydroxyl endgroup signals indicate there exists another initiation mechanism. According to the mechanism developed by Hoffmann and others (1, 9), hydroxyl radical can be produced through trapping the hole by water. The reaction is described as following equation:

$$h_{cb}^+ + H_2O \longrightarrow H^+ + {}^\bullet OH \tag{5}$$

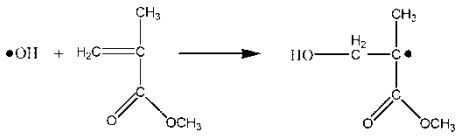

(6)

When the hole scavenger is added into the reacting system, methanol initiates efficient hole transfer from the oxygen lattice to the methanol. Then the methanol radical induces electron injection into TiO_2 with formation of surface-trapped electrons and formaldehyde (11–13).

$$CH_3OH + h^+_{cb} \longrightarrow H^+ + {}^\bullet CH_2OH \quad (7)$$

$${}^\bullet CH_2OH + Ti^{IV}{-}O{-}Ti^{IV}{-}OH \longrightarrow Ti^{IV}{-}O{-}Ti^{III} + CH_2O + H_2O \quad (8)$$

Therefore, e^-_{cb} is chiefly responsible for the polymerization when the hole scavenger is added. It has been proven that the hydroxyl radical can be generated from valence-band electron e^-_{cb} in gaseous solution. The electron is trapped by the primary hydrated surface of nano-TiO_2 ($Ti^{IV}OH$), thereafter an $\{>Ti^{III}OH\}$ (as electron donor) is formed by interfacial charge transfer. The subsequent reduction of the electron donor with O_2 produces a charge carrier of $O_2^{\bullet -}$. Commencing with $O_2^{\bullet -}$, OH-radical is generated through the following sequences (1,9):

$$e^-_{cb} + >Ti^{IV}OH \longrightarrow \{>Ti^{III}OH\} \quad (9)$$

$$\{>Ti^{III}OH\} + O_2 \longrightarrow O_2^{\bullet -} \quad (10)$$

$$H^+ + O_2^{\bullet -} \longrightarrow HOO^\bullet \quad (11)$$

$$2HOO^\bullet \longrightarrow H_2O_2 + O_2 \quad (12)$$

$$O_2^{\bullet -} + H_2O_2 \longrightarrow O_2 + OH^- + {}^\bullet OH \quad (13)$$

It appears that the hydroxyl radical is responsible for the initiation of polymerization in the presence of the hole scavenger. The addition reaction of the hydroxyl radical and MMA produces a monomer radical, as described by Reaction 6. Thus, the different phenomenon of three reaction modes can be reasonably explained. In the reaction mode A as blank experiment, either the valence-band hole or conduction-band electron can evolve into the initiation radicals. When adding a hole scavenger in the reaction mode B, the conduction-band electron can mostly possess the initiation of polymerization (Reactions 9–13). When adding electron scavenger in the reaction mode C, the initiation step from the valence-band hole rule the dominant status (Reactions 2–5). In this case, the polymer products have both the unsaturated double bond and hydroxyl group as the endgroups.

Conclusions

The additions of charge scavengers into the photopolymerization can synthesize the polymer with different polymer structures. It is approved that the products made by different charge scavengers have various properties such as molecular weight, macromolecular structure, molecular weight distribution, stereoregularity of chains, glass transition temperature and thermal degradation temperature. Our results suggest that there are two different mechanisms in the photopolymerization system. In the reaction without adding scavenger, either the valence-band hole or conduction-band electron can evolve into the initiation radicals. When adding hole scavenger, the conduction-band electron can mostly possess the initiation of polymerization. When adding electron scavenger, the initiation step from the valence-band hole rules the dominant status. To our knowledge, it is the first time separating the two different initiation mechanisms successfully by using the hole and electron scavengers, respectively.

The photopolymerization initiated by nano-TiO_2 semiconductor particles provides a novel method to prepare semiconductor/polymer nanocomposites via the initiation of the semiconductor itself. The results of this work will assist in the development of the nanocomposites with proper polymer structures.

Acknowledgements

We are grateful to the Shanghai Nanotechnology Promotion Center (SNPC) for financial support.

References

1. Hoffmann, M.R., Martin, S.T., Choi, W., and Bahnemann, D.W. (1995) Environmental Applications of Semiconductor Photocatalysis. *Chem. Rev.*, 95: 69.
2. Ngamsinlapasathian, S., Sakulkhaemaruethai, S., Pavasupree, S., Kitiyanan, A., Sreethawong, T., Suzuki, Y., and Yoshikawa, S. (2004) Highly Efficient Dye-Sensitized Solar Cell Using Nanocrystalline Titania Containing Nanotube Structure. *J. Photochem. Photobiol. A Chem.*, 164: 145.
3. Wang, R., Hashimoto, K., Fujishima, A., Chikuni, M., Kojima, E., Kitamura, A., Shinohigoshi, M., and Watanabe, T. (1997) Light-Induced Amphiphilic Surfaces. *Nature*, 388: 431.
4. Hoffman, A.J., Yee, H., Mills, G., and Hoffmann, M.R. (1992) Photoinitiated Polymerization of Methyl Methacrylate Using Q-Sized ZnO Colloids. *J. Phys. Chem.*, 96: 5540.
5. Hoffman, A.J., Mills, G., Yee, H., and Hoffmann, M.R. (1992) Q-Sized CdS: Synthesis, Characterization, and Efficiency of Photoinitiation of Polymerization of Several Vinylic Monomers. *J. Phys. Chem.*, 96: 5546.
6. Huang, Z.Y., Barber, T., Mills, G., and Morris, M.B. (1994) Heterogeneous Photopolymerization of Methyl Methacrylate Initiated by Small ZnO Particles. *J. Phys. Chem.*, 98: 12746.
7. Popovic, I.G., Katslkas, L., Muller, U., Velickovic, J.S., and Weller, H. (1994) The Homogeneous Photopolymerization of Methyl Methacrylate by Colloidal Cadmium Sulfide. *Macromol. Chem. Phys.*, 195: 889.
8. Stroyuk, A.L., Granchak, V.M., Korzhak, A.V., and Kuchmii, S.Ya. (2004) Photoinitiation of buthylmethacrylate polymerization by colloidal semiconductor nanoparticles. *J. Photochem. Photobiol. A Chem.*, 162: 339.
9. Dong, C. and Ni, X.Y. (2004) The Photopolymerization and Characterization of Methyl Methacrylate Initiated by Nanosized Titanium Dioxide. *J. Macromol. Sci. Pure and Applied Sci.*, 41: 547.
10. McCaldin, J.O. (1998) Semiconductors Interfacing Polymers for Light Emission. *Prog. Solid St. Chem.*, 26: 241.
11. Micic, O.I., Zhang, Y.N., Cromack, K.R., Trifunac, A.D., and Thurnauer, M.C. (1993) Photoinduced Hole Transfer from TiO_2 to Methanol Molecules in Aqueous Solution Studied by Electron Paramagnetic Resonance. *J. Phys. Chem.*, 97: 13284.
12. Rajh, T., Ostafin, A.E., Micic, O.I., Tiede, D.M., and Thurnauer, M.C. (1996) Surface Modification of Small Particle TiO_2 Colloids with cysteine for Enhanced Photochemical Reduction: An EPR Study. *J. Phys. Chem.*, 100: 4538.
13. Hurum, D.C., Agrios, A.G., Gray, K.A., Rajh, T., and Thurnauer, M.C. (2003) Explaining the Enhanced Photocatalytic Activity of Degussa P25 Mixed-Phase TiO2 Using EPR. *J. Phys. Chem. B.*, 107: 4545.
14. Beydoun, D., Tse, H., Amal, R., Low, G., and McEvoy, S. (2002) Effect of Copper(II) on the Photocatalytic Degradation of Sucrose. *J. Mol. Catala. A Chem.*, 177: 265.
15. Foster, N.S., Noble, R.D., and Koval, C.A. (1993) Reversible Photoreductive Deposition and Oxidative Dissolution of Copper Ions in Titanium Dioxide Aqueous Suspensions. *Environ. Sci. Technol.*, 27: 350.

16. Yu, T.Y. (1995) Free Radical Polymerization. In *Polymer Chemistry*, 1st Ed.; Shanghai, P.R., ed.; Fudan University Press: China; Vol. 4, 99.
17. Cameron, G.G. and Kerr, G.P. (1968) Simultaneous Occurrence of Chain-end and Random Initiation During Thermal Degradation of Poly(methyl methacrylate). *Makromol. Chem.*, 115: 268.
18. Fox, T.G. and Flory, P.J. (1954) The Glass Temperature and Related Properties of Polystyrene. Influence of Molecular Weight. *J. Polym. Sci.*, 14: 315.
19. Zhang, W., Li, Y., Wei, L., and Fang, Y. (2003) *In situ* Intercalative Polymerization of Poly(methylmethacrylate)/Clay Nanocomposites by Gamma-Ray Irradiation. *Mater. Lett.*, 57: 3366.
20. Carriere, P., Grohens, Y., Spevacek, J., and Schultz, J. (2000) Stereospecificity in the Adsorption of Tactic PMMA on Silica. *Langmuir*, 16: 5051.
21. Hatada, K. (1999) Stereoregular Uniform Polymers. *J. Polym. Sci. A Polym. Chem.*, 37: 245.
22. Kitayama, T., Janco, M., Ute, K., Niimi, R., Hatada, K., and Berek, D. (2000) Analysis of Poly(ethyl methacrylate)s by On Line Hyphenation of Liquid Chromatography at the Critical Adsorption Point And Nuclear Magnetic Resonance Spectroscopy. *Anal. Chem.*, 72: 1518.
23. Peters, R., Mengerink, Y., Langereis, S., Frederix, M., Linssen, H., van Hest, J., and van der Wal, S.J. (2002) Quantitation of Functionality of Poly(methyl methacrylate) by Liquid Chromatography Under Critical Conditions Followed by Evaporative Light-Scattering Detection Comparison with NMR and Titration. *J. Chromatogr. A*, 949: 327.
24. Tatro, S.R., Baker, G.R., Bisht, K., and Harmon, J.P. (2003) A MALDI, TGA, TG/MS, and DEA Study of the Irradiation Effects on PMMA. *Polymer*, 44: 167.
25. Dong, L.M., Hill, D.J.T., O'Donnell, J.H., Carswell-Pomerantz, T.G., Pomery, P.J., and Whittaker, A.K. (1995) Investigation of High-Temperature Radiation Effects on Poly(methyl methacrylate) of Specific Tacticity. *Macromolecules*, 28: 3681.
26. Podesva, J., Dybal, J., Spevacek, J., Stepanek, P., and Cernoch, P. (2001) Supramolecular Structures of Low-Molecular-Weight Polybutadienes, as Studied by Dynamic Light Scattering, NMR and Infrared Spectroscopy. *Macromolecules*, 34: 9023.